Journal of Environmental Science International
25(10); 1433~1444; October 2016

pISSN: 1225-4517 eISSN: 2287-3503
http://dx.doi.org/10.5322/JESI.2016.25.10.1433

ORIGINAL ARTICLE

Assessment of Sediment Yield according to Observed Dataset

Sangeun Lee, Sanghyeok Kang[1)*]

Department of Energy and Mineral Resources Engineering, Kangwon National University, Samcheok 25913, Korea
[1)]*Department of Civil Engineering, Kangwon National University, Samcheok 25913, Korea*

Abstract

South Korea is a maritime nation, surrounded by water on three sides; hence, it is important to preserve in a sustainable manner. Most areas, especially those bordering the East Sea, have been suffering from severe coastal erosion. Information on the sediment yield of a river basin is an important requirement for water resources development and management. In Korea, data on suspended sediment yield are limited owing to a lack of logistic support for systematic sediment sampling activities. This paper presents an integrated approach to estimate the sediment yield for ungauged coastal basins by using a soil erosion model and a sediment delivery rate model in a geographic information system (GIS)-based platform. For applying the sediment yield model, a basin specific parameter was validated on the basis of field data, that, ranging from 0.6 to 1.2 for the 19 gauging stations. The calculated specific sediment yield ranged from 17 to 181 t/km^2.yr in the various basin sizes of Korea. We obtained reasonable sediment yield values when comparing the measured data trends around the world with those in Korean basins.

Key words : Monsoon region, Sediment delivery rate, Sediment yield, Modeling

1. Introduction

South Korea (S. Korea) is surrounded by sea on three sides, with 11,542 km of coastline. Most beaches on the west coast are clayey tidal flats. The tide is semidiurnal with maximum range of about 10 m. The South Sea is a group of islands adjacent to Japan. On the other hand, most beaches on the east coast are sandy beaches that have been suffering from beach erosion. The coastal region is the most dynamic part of the seascape since its shape is affected by various factors, such as hydrography, geology, climate, and vegetation. Coastal erosion may be caused by natural processes such as waves, currents, and storms as well as human activities such as land reclamation, recreation at beaches, and construction of infrastructure in coastal areas (Rosati, 2005).

In connection with the coastal erosion, Philips (Phillips, 1995) has pointed out that rivers are the major source of coastal sediment. Natural river reaches are usually in a state of morphological equilibrium in coastal areas, where the sediment inflow on average balances the sediment outflow.

The sediment in coastal areas represents evidence of changes from river sediment delivery driven by human or natural impacts. Urbanization affects this

Received 9 October, 2016; **Revised** 21 October, 2016;
Accepted 21 October, 2016
[*]**Corresponding author** : Sanghyeok Kang, Department of Civil Engineering, Kangwon National University, Samcheok 25913, Korea
Phone : +82-33-570-6570
E-mail : kang7231@hanmail.net

ⓒ The Korean Environmental Sciences Society. All rights reserved.
This is an Open-Access article distributed under the terms of the Creative Commons Attribution Non-Commercial License (http:// creativecommons.org/licenses/by-nc/3.0) which permits unrestricted non-commercial use, distribution, and reproduction in any medium, provided the original work is properly cited.

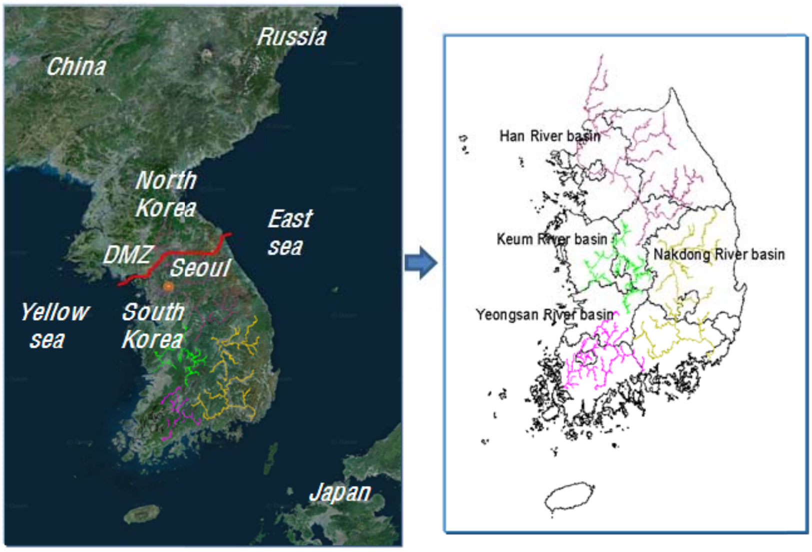

Fig. 1. Study area and location of the four major basins.

equilibrium by decreasing, slowing, and halting the movement of sediment to coastal areas. This is an important issue for many coastal regions around the world (Kurt, 2010). It is also becoming increasingly obvious that sediment loads in the world's rivers have been impacted by human development. Unfortunately, in practice sediment yield (SY) data are very limited in these areas due to lack of high cost sediment data collection. This paper aims to estimate annual potential soil erosion, sediment delivery rate and SY based on measured data. Additionally, specific objectives were (ⅰ) to present a methodology that combines GIS with RUSLE and a sediment transport model to estimate the spatial distribution of soil erosion and SY at a basin scale, and (ⅱ) to demonstrate the use of this methodology by applying it to gauging river basins.

2. Materials and Method

2.1. Study area and data collection

South Korea (Korea) is located on the southern part in the Korean Peninsula in East Asia (Fig. 1). The approximate coordinates are 37° North, 127° 30 East. The only country with a land border to is North Korea, lying to the north with 238 kilometers of border running along the demilitarized zone (DMZ).

Korea is mostly surrounded by water and has 2,413 kilometers of coast line along three seas. To the west is the Yellow Sea, to the south is the East China Sea, and to the east is Ulleung-do. Geographically, Korea's land mass is approximately 100,032 km^2. Korea has four large rivers; the Han, Nakdong, Keum, and Yeongsan rivers. These river basins occupy 86 percent of the total Korea land area of 100,210 km^2. Korea has a continental climate with dry cold winters and hot humid summers. The annual mean rainfall is 1,248 mm, which varies by region and typhoon. Precipitation is the major source of sediment load in Korea. Korea receives approximately two thirds of its annual precipitation during the summer monsoon season from July to September. Changes in the timing and amount of precipitation could lead to flood hazards. Attacks from typhoons sometimes caused a great deal of damage to the region. In order to analyze the characteristics of soil erosion within the basin and the cause of SY, a soil erosion model requires information on the digital elevation model (DEM), soil, and land cover. To determine the geomorphological characteristics, we developed a triangle irregular network (TIN) using a 1:5,000 scale digital topographic map crafted by the national geographic information institute (NGII). Using the TIN, a 10 m resolution DEM was developed because it is closest to the typical revised universal soil loss equation (RUSLE) resolution of 22 m. The land cover data was processed using 30 m resolution LANDSAT satellite images by water management information system (WAMIS, 2015).

2.2. Mechodology

2.2.1. Soil erosion

RUSLE is used as a soil erosion model to estimate the amount of soil erosion from basins (Wischmeier and Smith, 1978).

As the theoretical basis of RUSLE has been clearly reported elsewhere (Kinnell, 2008), we provide here only a brief description of the model. In the RUSLE, the amount of soil loss is a product of five factors representing the rainfall and basin characteristics, as follows;

$$A_{Ei} = R_i \cdot \ K_i \cdot \ LS_i \cdot \ C_i \cdot \ P_i \tag{1}$$

Where A_{Ei} is the gross amount of soil erosion in i^{th} cell (ton/ha.yr); R is the rainfall runoff erosivity factor (MJ mm/ ha.h.year); K is the soil erodibility factor (ton/ha/R); LS represent slope length and slope steepness (dimensionless); C is the cover management factor (dimensionless); and P is the supporting practice factor (dimensionless).

Rainfall Erosivity factor, R is generally calculated from an annual summation of rainfall data using rainfall energy over 30-min duration. On annual basis, the products of precipitation's total kinetic energy per unit area, EI30 value is the sum of values over the storms in an individual year. The erosivity of rainfall varies greatly by location because of the effects of elevation in rainfall. Wischmeier and Smith (Wischmeier and Smith, 1958) observed that there's a high correlation between rainfall kinetic energy and its maximum intensity, EI30 and the amount of soil eroded. Erosivity factor is an indication of the two most important characteristics of a storm determining its erosivity: amount of rainfall and peak intensity sustained over an extended period.

Some researchers evaluated the erosivity and developed statistical relationship between R-factor and the total annual precipitation (Pal et al., 2012) As there are limited meteorological stations in mountainous basin, information on rainfall amount and pattern needs to be assumed based on neighboring stations (Lee and Kang, 2013). The rainfall information available represents point data, and this has to be extrapolated in terms of spatial distribution, using the Arc GIS contouring function. In this study, the Equation 2, developed by Korea Institute of Construction Technology (KICT, 1992), was used for computing the R factor as:

$$R = 38.5 + 0.35 \times P_r \tag{2}$$

where, P_r is the average annual precipitation of the study area.

The erodibility of a soil K is an expression of its inherent resistance to detachment and transport by rainfall (Wischmeier et al., 1971). It is determined by the cohesive force between the soil particles. Soil erodibility may vary depending on soil characteristics, such as particle distribution, soil structure, and organic matter, etc. The formula for soil erodibility (Kamaludin et al., 2013) is as follows:

$$K = \frac{2.1 \times 10^{-4}(12 - OM\%)(N1 \times N2)^{1.14} + 3.25(SS - 2) + 2.5(PP - 3)}{100} \tag{3}$$

where *OM* is organic matter (%), *N*1 is clay+very fine sand (0.002 – 0.125 mm), *N*2 is clay+very fine sand+sand (0.125 – 2 mm), *SS* is soil structure code (Wischmeier and Smith, 1978), and *PP* is profile permeability class (Wischmeier and Smith, 1978).

Korean National Academy of Agricultural Science published the soil map with 1:50,000 scales (NAAS, 2014). Based on this map, a digital soil map was produced with the ArcGIS coverage of the 1:25,000 scales. Soil classification in study area was divided into 59 types of total 390 soil types.

LS are the slope length and gradient factor. The slope length and slope steepness can be used in a single index, which expresses the ratio of soil loss as defined by Wischmeier and Smith(1978) as:

$$LS = (X/22.1)^{m} (0.065 + 0.045 S + 0.0065 S^2) \quad (4)$$

where, *X* is the slope length (m), *m* is slope length exponent, and *S* is slope gradient (%). In order to calculate *X* value, Flow Accumulation was derived from DEM after conducting Fill and Flow Direction processes in ArcGIS. The vegetation cover factor *C* represents the ratio of soil loss under a given vegetation cover as opposed to that on bare soil. The vegetation cover intercepts raindrops and dissipates its kinetic energy before it reaches the ground surface (Renard et al., 1997). The relative impact of management options can easily be compared by making changes in the C factor which varies from near zero for well protected land cover to one for the barren areas (Lee and Lee, 2006). The effect of contouring and tillage practices on soil erosion is described by the support practice factor *P* within the RUSLE model (Renard et al., 1997). Wischmeier and Smith(1978) defined the support practice factor *P* as the ratio of soil loss with a specific support practice to the corresponding soil loss due to up and down cultivation. If there are no support practices, the *P* factor is 1.00. Contemporary agricultural practices consist of up and down tillage without the presence of contours, strip cropping, or terracing. The P factor depends on the conservation measure applied to the study area. In this study, the factors C and P were applied on the basis of KICT(1992) classification.

2.2.2. River sediment yield model

SY is the amount of solid particles that is delivered to the outlet of the basin. SY at a mouth of the basin is calculated by multiplying gross erosion above that point by a SDR (sediment delivery rate). The SY load from each measurement can be derived as:

$$Q_{ss} = 0.0864 Q \cdot C_s \quad (5)$$

where Q_{ss} is suspended sediment load (t/day), Q is water discharge (m^3/s), C_s is sediment concentration (mg/ L)

Calculating the annual sediment load of a river can be quite straightforward, if discharge and sediment concentration are measured at closely spaced intervals, particularly during floods. In most cases, however, a continuous record of sediment concent -ration is not available, and indirect methods must be utilized using a sediment rating curve (SRC). The SRC is a widely adopted method for estimating sediment concentration and load (Yekta et al., 2010).

As sediment concentration and load often vary over several orders of magnitude, the SRC is generally established by a power function (Lu and Siew, 2005) that relates available sediment load (Q_s) to water discharge (Q):

$$Q_s = aQ^b \quad (6)$$

where *a* is regression constant and *b* is slope by regression analysis.

2.2.3. Review of sediment delivery rate

The SDR is the ratio of SY at the outlet, over the total volume of produced sediment using Eq. (5) in the drainage basin. It is well known that the SDR is related to basin size, i.e. it decreases with the size of basin. There are some methods to estimate SDR, namely an observed SRC model linking RUSLE, and a combination of the sediment delivery distribution (SEDD) model and RUSLE model (Lee and Kang, 2014). The SDR values can be assessed with GIS-based spatially distributed sediment models using field experimental data.

2.2.4. SDR model coupling RUSLE and SRC

RUSLE is a basin model; thus it cannot be directly used to estimate the amount of sediment reaching downstream areas, because some portion of the eroded soil may be deposited while traveling to the watershed outlet or the downstream point of interest (Neibling and Foster, 1977). To account for these processes, the SDR for a given watershed should be used to estimate the total sediment transported to the watershed outlet. The SDR can be expressed as follows:

$$SDR = SY/A_E \tag{7}$$

where SDR is the sediment delivery ratio; SY is the sediment yield; and A_E is the gross erosion for the entire watershed.

2.2.5. Sediment delivery distribution (SEDD) model

Empirical Equations for SDR are usually based on variables, such as basin area, slope and land cover (Ferro and Porto, 2000). For example, Kothyari and Jain (Kothyari and Jain, 1997) estimated the SDR values from the watershed area, relief ratio and average runoff curve number value. They applied a lumped approach, but improved this by division of the modeled basin into smaller watersheds. According to some authors (Mutua and Klik, 2006), the coefficient, which is a measure of the probability that the eroded particles are transferred from the morphological unit under consideration to the nearest stream reach, can be generalized as follows:

$$SDR_i = \exp(-\gamma t_{P,i}) = \exp\left[\sum_{i=1}^{N_P} \frac{l_i}{v_i}\right] = \exp\left[-\gamma\left(\sum_{i=1}^{N_P} \frac{l_i}{a_i \cdot \ s_i^{0.5}}\right)\right] \tag{8}$$

where γ is basin specific parameter depends on morphological data, $t_{P,i}$ is travel time (hr) of overland flow from the *i*th overland cell to the nearest channel cell down the drainage path.

If the flow path from cell i to the nearest channel traverses *Np* cells, then the travel time from that cell is calculated by adding the travel time for each of the *Np* cells located along the flow path.

$l_{P,i}$ is the length of segment *i* in the flow path (m), and is equal to the length of the side or diagonal of a cell, depending on the flow direction in the cell. v_i is the flow velocity for the cell (m/s). The flow velocity is considered to be a function of the land surface slope and the land cover characteristics (Wu et al., 2003) i.e. $v_i = a_i \times S_i^b$. If A_E is the amount of soil erosion produced within the i^{th} cell of the basin estimated using Equation 1, then the SY for the basin, SY, is obtained, as below:

$$SY = \sum_{i=1}^{n} SDR \cdot \ A_E \tag{9}$$

where *n* is the total number of cells over the basin, and the term SDR is the fraction of S_E that ultimately reaches the nearest channel. Since the SDR of a cell is hypothesized as a function of travel time to the nearest channel, this implies that the gross erosion in that cell multiplied by the SDR value of the cell becomes the SY contribution of that cell to the nearest stream channel. The SDR values for the cells marked as

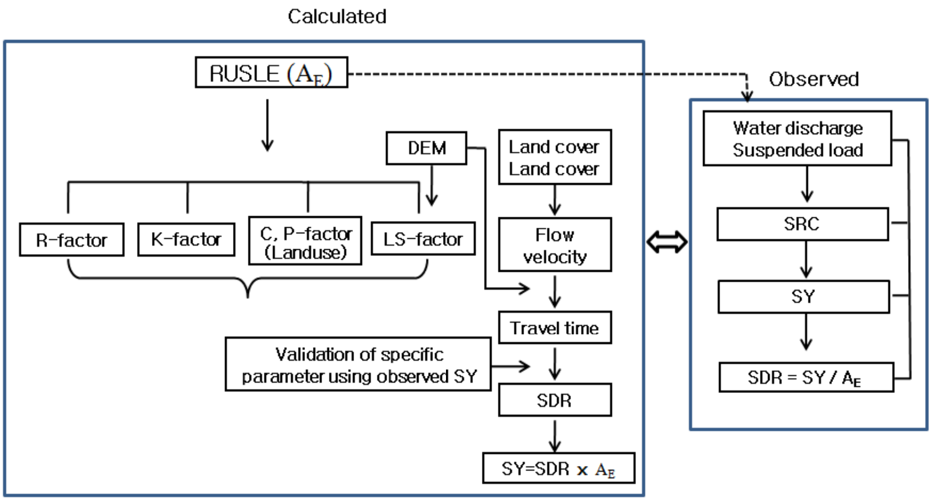

Fig. 2. Model validation process between calculated and observed sediment yields using model builder of ArcGIS.

channel cells are assumed to be unity. SY modeling is a more complicated and time-consuming process, since the RUSLE method cannot drive the SY directly. In order to estimate the SY, then we combine the RUSLE and SDR model, using the model builder (MB) in the ArcGIS environment. Simulated SY was validated with observed one as shown in Fig. 2.

3. Results and Discussion

3.1. Soil erosion

In order to calculate SDR by modeling, the relationship between soil loss and SY needs to be determined. The annual soil erosion from each identified grid of the two basins was computed by integration of the RUSLE erosion factors, namely *R*, *K*, *LS*, *C* and *P* of RUSLE. The values of the RUSLE parameters were integrated in ArcGIS, using a Raster Calculator to form a composite map denoting gross soil erosion, based on 30 m DEM. Land use data of 30 x 30 m, provided by the water management information system (WAMIS), was reclassified to create a new map with the following categories: (a) water, (b) urban, (c) barren, (d) wetland, (e) pasture, (f) forest, (g) paddy farming, and (h) field crop area. The soil classification map of the study area was divided into 59 soil types such as Afa, Ana, Apa, Rea, Maa, Ro, etc. In 1973, the NAAS published the soil map at a scale of 1:50,000. Based on this paper map, a digital soil map was produced with the ArcGIS coverage of a 1:25,000 scale. Rainfall erosivity is determined by climatic data. For calculating R factors in the study basins, we used an annual average value using the isohyetal method based on 59 meteorological observation stations (Lee and Kang, 2013).

Changes occurring in the values of the factor *C* due to crop growth over such a small duration were neglected (Mutua and Klik, 2006). In this study, the factors C and P were applied on the basis of KICT(1992) classification.

Potential annual soil loss (*A*) value was computed by overlaying five grid surfaces over the 19 study basins. The grid surfaces represented the values of rainfall erosivity factor (*R*), cover management factor (*C*), soil erodibility factor (*K*), topographic factor (LS) and practice management factor (*P*). The annual soil

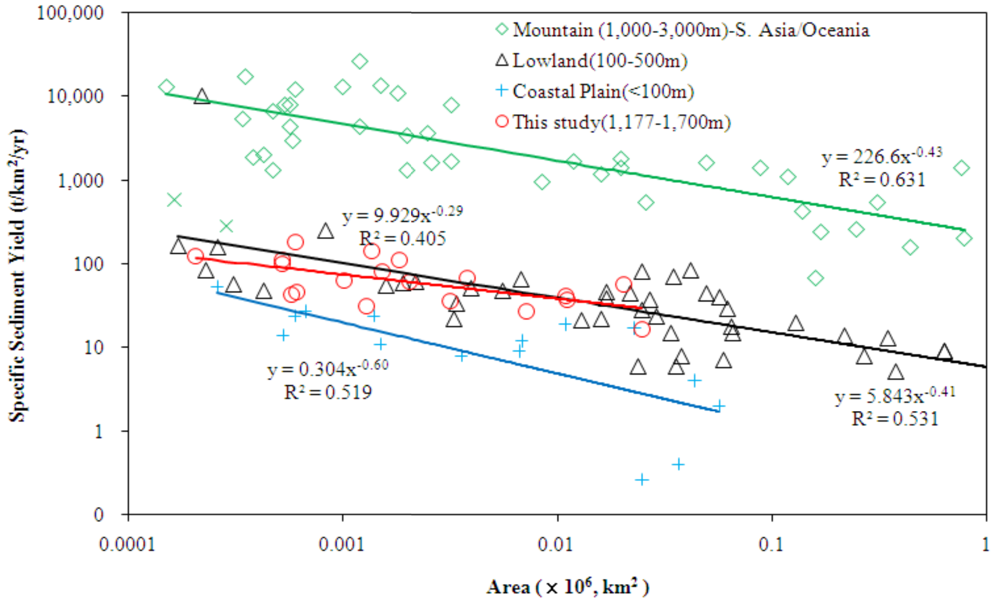

Fig. 3. Specific sediment yield with Milliman and Syvitski(1992).

loss values obtained for the study basins ranged from 197 to 793 ton/km^{-2}.yr.

3.2. Sediment yield

Although SY is defined as the total sediment load discharged from a basin, the bed load component is usually ignored and SY is equated with the outflow of suspended sediment. SY is usually less than the amount of soils actually eroded in the river basin. It is normally expressed as the total sediment volume delivered to a specified location in the basin, typically the river mouth, divided by the effective drainage area above that location for a specified period of time. In order to estimate the annual SY, a SRC using Equation (6) was derived as a linear regression, on the basis of field measured data, during the period from 2011 to 2015. The regression approach can provide good results for the prediction of the annual sediment load in streams with large drainage basins. The approach may also give good results for the prediction of the daily sediment load in streams of small and homogeneous drainage basins. Some investigators even suggest the use of linear regression for drainage basins without sediment records to obtain an order-of-magnitude estimate of SY (Fernandez et al., 2003; Fu et al., 2006).

For deriving SRC, we used data classification method to show the relationship between incoming sediment discharge and water discharge. Table 1 shows rating relationships developed in the 19 gauging stations. All fieldwork was carried out during the rainy seasons during from July to September of 2008 – 2014. In monsoon region, sampling flash flood is dangerous and difficult since flow depths increase very rapidly during the rising limb of the floods. In this study, it was observed that the Q – relationship is generally good when all samples of a gauging station are considered. It was noted that for a given Q, is generally much higher at the start of the rainy season than toward the end. Therefore, for each studied catchment, samples of all measuring campaigns were combined for driving SRC.

In general, the total sediment load is often estimated by measuring suspended load, while the bedload fraction is neglected due to constraints (Milliman and Syvitski, 1992). The distribution of mean SY is skewed to higher values, that is to say from 17 to 181 t km^{-2} $year^{-1}$ with the different size of basin area as shown in Table 2. These SSY values are similar to previous research in lowland area or present a somewhat lower load with similar size of headwater basin than that of other South Asia/Oceania rivers (Milliman and Syvitski, 1992), as shown in Fig. 3.

This lower runoff of SSY mainly reflects topographical geological and hydrological effects. The hydrographs of the water discharge in Korea are very sharp, and peak discharges are very large compared with continental rivers because of the topographical conditions and occasional torrential rainfall, but seldom contain extensive SY, except for the monsoon period. Most of total SY is concentrated in monsoon period from June to September (Table 2).

3.3. Validation of sediment delivery rate

The cell-based SDR allows the identification of critical sediment source and delivery areas as well as the site-specific implementation of proper management practices within a basin. It is noted that the SDRs imply the integrated capability of a basin for storing and transporting the potential eroded soil.

The SDR in the i^{th} cell of Equation (8) represents the soil loss from cell i that actually reaches a continuous stream system. The SDR was estimated following the definition given by Kothyari and Jain (Kothyari and Jain, 1997), which is a function of travel time. Flow velocity in reality is controlled by

Table 1. Overview of sediment rating curves for 19 study basins

Basin	Gauging station	Area (km^2)	Equation	a	b	R^2	n
Han_R	CM	525	$Q_S = aQ^b$	0.255	1.872	0.868	51
	MM	1,359		0.017	2.066	0.867	54
	YJ	11,104		0.003	2.082	0.846	55
	Han-R	24,753		0.008	1.655	0.981	14
Nakdong_R	JC	608		4.155	0.989	0.610	25
	SSan	1,006		0.312	1.643	0.882	52
	YG	1,287		0.531	1.449	0.920	28
	HS	1,530		1.823	1.344	0.781	66
	JA	3,181		0.639	1.324	0.755	76
	WK	10,992		0.023	1.852	0.825	48
	JD	20,311		0.126	1.568	0.847	83
Kuem_R	KR	206		0.006	2.670	0.988	15
	HD	601		0.187	1.838	0.904	31
	HG	1,831		0.540	1.573	0.883	20
	KJ	7,149		0.012	2.047	0.895	77
Youngsan_R	SA	525		0.055	1.885	0.910	30
	NP	576		0.076	1.872	0.936	69
	NJ	2,059		0.082	1.819	0.858	98
	KR2	3,810		0.020	1.955	0.972	56

Notes : CM: Chengmi; MM: Munmak; YJ: Yeaju; Han-R: Han River; JC: Jeomchon; SSan: Sunsan; YG: Yanggok; HS: Hyangsuk; JA: Jungam; WK: Weakwon; JD: Jindong; KR: Kuryoung; HD: Headuk; HG: Hapgang; KJ: Kongju; SA: Sunam; NP: Nampyeng; NJ: Naju; KR2: Kurae 2

Table 2. Sediment yield including monsoon season in 19 gauging stations

Basin	Gauging station	Area (km^2)	Annual load							Monsoon season	
			2011	2012	2013	2014	2015	Mean SY(t)	SSY (t/km^2)	Mean SY(t)	% of annual
Han_R	CM	525	-	-	55,803	-	60,405	58,104	111	55,607	96
	MM	1,359		186,131	110,756	389,046	82,267	192,050	141	188,687	98
	YJ	11,104	210,416	678,338	388,545		366,003	410,826	37	382,347	93
	Han-R	24,753	-	-	263,221	785,362	179,846	409,476	17	374,814	92
Nakdong_R	JC	608	-	-	22,802	32,975	26,926	27,568	45	19,888	72
	SSan	1,006	-	-	68,618	57,289	68,114	64,674	64	62,411	97
	YG	1,287	-	-	34,723	47,035		40,879	32	34,532	84
	HS	1,530	-	-	80,570	199,483	94,637	124,897	82	102,090	82
	JA	3,181	-	-	103,901	134,331	106,930	115,054	36	91,880	80
	WK	10,992	309,222	380,817	691,591			460,543	42	404,381	88
	JD	20,311	-	564,347	897,977	1,878,390	1,353,119	1,173,458	58	1,016,737	87
Kuem_R	KR	206	-	-	16,202	35,380	-	25,791	125	25,760	97
	HD	601	-	-	30,231	218,487	76,990	108,569	181	105,980	98
	HG	1,831	-	-	196,723	-	209,306	203,015	111	180,913	89
	KJ	7,149	119,559	176,327	288,989	-	-	194,958	27	176,807	91
Youngsan_R	SA	525	-	-	116,577	16,552	23,560	52,230	99	49,076	94
	NP	576	-	-	24,415	-	-	24,415	42	22,444	92
	NJ	2,059	62,678	-	189,167	-	-	125,923	61	110,347	88
	KR2	3,810	375,575	13,839	327,638	323,578	273,323	262,791	69	257,841	98

conditions such as surface vegetation type and roughness, and elevation changes over the basin. It means that longer travel times tended to occur in areas with rougher surfaces like a vegetated area compared to areas with impervious and open land surfaces. It is well known that an inverse relationship exists between SDR and the basin area. SDR generally increases with decreasing basin size. The SDR in the field approaches 100% for small and urbanized basins (Walling, 1983). We derived a similar result that calculated SDR increases with decreasing basin size.

The sensitivity of the coefficient appearing in Equation (8) for SDR was studied empirically Ferro and Porto (Ferro and Porto, 2000). Kothyari and Jain(1997) reported that the SY is not very sensitive to the value. On the other hand, Mutua and Klik(2006) asserted that SDR was very sensitive to the value. Despite these different findings, the value is treated as a constant parameter. In order to estimate the sensitivity of the basin specific parameter (γ), simulated SY was compared with observed one. We found that the SDR simulated was ranged from 0.04 to 0.38 with ranged from 0.03 to 0.53 for observed one.

At that time, the γ values were range from 0.6 to 1.2. A good agreement between measured and calculated SY values was obtained, validating the model by a specific parameter for each basin. This indicates that these efforts will help to estimate the SY for ungauging basins. It is, however, insisted that the river basins vary greatly in size and topographic condition, and that SDR calculation methods vary

Table 3. Calculated results of sediment yield (SY), sediment delivery rate (SDR) and specific parameter (γ) based on observed dataset

Basin	Gauging station	Area (km^2)	A (t/yr)	Observed		Simulated		
				SY (t)	SDR	SY (t)	SDR	γ
Han_R	CM	525	110,000	58,104	0.53	570,000	0.38	0.7
	MM	1,359	610,000	192,050	0.31	190,000	0.25	0.7
	YJ	11,104	8,800,000	410,826	0.05	430,000	0.06	0.9
	Han-R	24,753	13,000,000	409,476	0.03	420,000	0.04	0.8
Nakdong_R	JC	608	120,000	27,568	0.23	30,000	0.20	0.6
	SSan	1,006	646,099	64,674	0.10	61,000	0.21	0.6
	YG	1,287	487,786	40,879	0.08	43,000	0.20	1.2
	HS	1,530	1,075,943	124,897	0.12	120,000	0.24	1.2
	JA	3,181	2,244,734	115,054	0.05	120,000	0.18	0.8
	WK	10,992	5,885,428	460,543	0.08	475,000	0.06	0.6
	JD	20,311	11,321,058	1,173,458	0.10	1,300,000	0.06	0.6
Kuem_R	KR	206	160,000	25,791	0.16	26,000	0.10	0.8
	HD	601	230,000	108,569	0.47	110,000	0.31	1.0
	HG	1,831	1,100,000	203,015	0.09	220,000	0.21	1.0
	KJ	7,149	5,180,000	194,958	0.04	215,000	0.10	1.2
Youngsan_R	SA	525	170,000	52,230	0.30	55,000	0.17	1.0
	NP	576	280,000	24,415	0.08	25,500	0.14	1.0
	NJ	2,059	610,000	125,923	0.20	120,000	0.15	0.8
	KR2	3,810	2,650,000	262,791	0.09	275,000	0.05	1.2

between studies, so any comparison must be made with careful concern. It will confirm that the accuracy of the SDR shown in this study strongly depends on the model selection for soil erosion, the quality of geospatial data, measurement accuracy, and basin characteristics.

4. Conclusions

The SY, especially in coastal areas, is too sensitive to readily obtain data. Their data has been scarcely used, because its conventional measurement methods are expensive and time-consuming. In this paper, a theoretically based relationship for evaluating the soil loss and SDR is proposed to estimate SY. Soil erosion in the individual cells of the basin was determined using the RUSLE. The value of SDR was calibrated comparing the calculated SY for the study basins and similar observed basins, as defined by equation (8). The annual SDR at the outlet of the basin was estimated in the range from 0.03 to 0.53 for the 19 gauging stations. The observed specific SY ranged from 17 to 181 $t/km^2.yr$. It is noted that modeling SY depends on calibration against a record of existing conditions and hence it can be used for the estimation of SY in other ungauged basins, which have similar hydro-meteorological and land cover conditions.

Acknowledgements

This study is supported by 2015 Research Grant from Kangwon National University (No. 201510039).

REFERENCES

Fernandez, C., Wu, J. Q., McCool, D. K., StÖckle, C. O., 2003, Estimating water erosion and sediment yield with GIS, RUSLE, and SEDD, Soil and Water Conser. Soci., 58(3), 128-136.

Ferro, V., Porto, P., 2000, Sediment delivery distri -bution (SEDD) model, J. of Hydrologic Engi., 5(4), 411-422.

Fu, G., Chen, S., McCool, D. K., 2006, Modeling the impacts of no-till practice on soil erosion and sediment yield with RUSLE, SEDD, and ArcView GIS, Soil & Tillage Res., 85, 38-49.

Kamaludin, H., Lihan, T., Ali Rahman, Z., Mustapha, M. A., Idris, W. M., Rahim, S. A., 2013, Integration of remote sensing, RUSLE and GIS to model potential soil loss and sediment yield (SY), Hydro Earth Sys. Sci Discuss., 10, 4567-4596.

Kinnell, P. I. A., 2008, Sediment delivery from hillslopes and the universal soil loss equation: Some perceptions and misconceptions, Hydrological Proc., 22, 3168-3175.

Korea Institute of Construction Technology (KICT), 1992, The development of selection standard for calculation method of unit sediment yield in river, 89-WR-113 Research Paper 1992 (in Korean).

Kothyari, U. C., Jain, M. K., 1997, Sediment yield estimation using GIS, Hydrological Sci. J., 46(6), 833-843.

Kurt, S., Karaburun, A., Demirci, A., 2010, Coastline change in Istanbul between 1987 and 2007, Scientific Res. and Essays, 5(19), 3009-3017.

Lee, G. S., Lee, K. H., 2006, Scaling effect for estimating soil loss in the RUSLE model using remotely sensed geospatial data in Korea, Hydrol Earth Syst. Sci. Discuss., 3,135 - 157.

Lee, S. E., Kang, S. H., 2013, Estimating the GIS -based soil loss and sediment delivery ratio to the sea for four major basins in South Korea, Wat. Sci. & Tech., 68(1), 124-133.

Lee, S. E., Kang, S. H., 2014, Geographic information system-coupling sediment delivery distribution modeling based on observed data, Wat. Sci. & Tech., 70(3), 495-501.

Lu, X. X., Siew, R. Y., 2005, Water discharge and sediment flux changes in the lower Mekong River, Hydrol. Earth Sys. Sci. Discuss., 2, 2287-2325.

Milliman, J. D., Syvitski, P. M., 1992, Geomorphic/ tectonic control of sediment discharge to the ocean: The importance of small mountainous rivers, The J. of Geol., 100, 525-544.

Ministry of Land, Infrastructure and Transport, 2015, Water Management Information System (WAMIS), Korea (in Korean).

Mutua, B. M., Klik, A., 2006, Estimating spatial sediment delivery ratio on a large rural catchment, J. of Spatial Hydrol., 6(1), 64-80.

National Academy of Agricultural Science (NAAS), 2014, Soil map, Korea, 2014 (In Korean).

Neibling, W. H., Foster, G. R., 1997, Estimating deposition and sediment yield from overland flow processes, International Symposium on Urban Hydrology, Hydraulics, and Sediment Control Procs. Univ. of Kentucky, Lexington.

Pal, B., Samanta, S., Pal, D. K., 2012, Morphometric and hydrological analysis and mapping for Watut watershed using Remote Sensing and GIS techniques, Int. J. of Adv. in Engi. & Tech., 2(1), 357-368.

Phillips, J. D., 1995, Decoupling of sediment sources in large river basins, effects of scale on interpretation and management of sediment and water quality, Proceedings a Boulder Symposium, July, IAHS publ. no. 226, 11-16.

Renard, K. G., Foster, G. R., Weesies, G. A., McCool, D. K., Yoder, D. C., 1987, Predicting soil erosion by water: A guide to conservation planning with the Revised Universal Soil Loss Equation (RUSLE).

Rosati, J. D., 2005, Concepts in sediment budgets, J. of Coastal Res., 21(2), 307-322.

US Department of Agriculture: Washington, DC, USA, 1997, Agriculture Handbook, 703.

Han River Flood Control Office, Water Resources Management Information System, 2016, http://www.wamis.go.kr/

Walling, D. E., 1983, The sediment delivery problem, J. Hydrol., 65, 209-237.

Wischmeier, W. H., Johnson, C. B., Cross, B. V., 1971, A soil erodibility nomograph for farmland and construction sites, J. Soil Water Conser., 26, 189-193.

Wischmeier, W. H., Smith, D. D., 1958, Rainfall energy and its relation to soil loss, Trans Am Geophys Union, 39(2), 285-291.

Wischmeier, W. H., Smith, D. D., 1978, Predicting Rainfall Erosion Losses, USDA Ag. Res. Serv. Handbook, 537, US Department of Agriculture: Washington, DC, USA.

Yekta, A. H. A., Marsooli, R., Soltana, F., 2010, Suspended sediment estimation of Ekbatan reservoir sub basin using adaptive neuro-fuzzy inference systems (ANFIS), artificial neural networks (ANN), and sediment rating curves (SRC), River Flow 2010, Dittrich, Koll, Aberle & Geisenhainer (eds), 807-813.